Numerical simulation of the production processes of layered materials

Gustavo J. Sibona[a,*], Sascha Schreiber[b], Ronald H.W. Hoppe[a], Bernd Stritzker[b], Adrian Revnic[a]

[a] *Institute of Mathematics, University of Augsburg, Augsburg 86159, Germany*
[b] *Institute of Physics, University of Augsburg, Augsburg 86159, Germany*

Abstract

Modeling of the production processes of layered materials can be done by molecular dynamics on the basis of an appropriate choice of interacting potentials of Tersoff-type, whose parameters are determined by ab initio methods. In particular, we analyze the ion beam assisted deposition of thin cubic boron nitride films and the co-deposition of fullerenes on silicon substrates. Numerical integration of the equation of motion is done by a parallel version of the Stoermer–Verlet scheme using a particle-in-cell method in addition to the nearest neighbor concept. Visualizations of the numerical simulations reveal a transition from hexagonal lattice to cubic crystallographic structures of the boron nitride layer, as observed in experiment. We also analyze in detail the fullerene-silicon substrate interaction by varying the impact energy and the angular speed of the fullerene molecule and the temperature of the system.

1. Introduction

The design of production processes for new materials with improved physical properties requires a subtle experimental setup, mathematical modeling, numerical simulation, and model validation by experimental data. In particular, a technologically relevant process in materials science is the coating of surfaces by thin films to produce innovative materials with tailored structural properties such as hardness and resistance to temperature and wear, playing a significant role in modern microelectronics, optoelectronics, and bearings.

An important field of application of these processes is in semiconductor technology, where new materials such as cubic boron-nitride (c-BN) and silicon carbide (SiC) are of utmost importance for constructing high power and high temperature devices due to their large bandwidth, high saturation drift velocity, high melting point, and excellent thermal conductivity (cf. Table 1).

The synthesis of c-BN by IBAD relies on a simultaneous physical vapor deposition and ion bombardment in a preparation chamber (see Fig. 1). A gas inlet provides the chamber with a mixture of N and an inert gas such as Ar. The gas is ionized by the electrons of a tungsten filament initiating a gas discharge. The electron beam evaporator, which has a maximal power of 4 kW [13], is in a water-cooled crucible made of graphite to avoid metallic pollution. At the same time, boron ions, typically gaseous, are simultaneously extracted from a plasma and accelerated into the growing PVD film at energies varying between 50 eV and 2 keV [15].

---

*Corresponding author. Tel.: +49-821-598-2192; fax: +49-821-598-2339.

E-mail address: sibona@math.uni-augsburg.de (G.J. Sibona).

Table 1
Characteristics and applications of c-BN and SiC

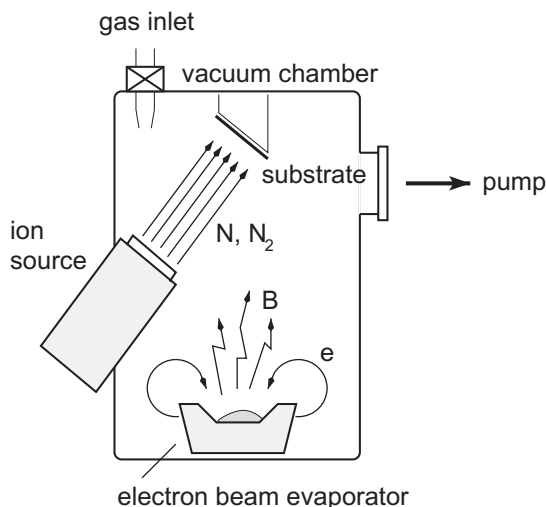| Characteristics/ applications	Cubic boron nitride	Silicon carbide
Hardness	70–90 GPa	40–65 GPa
Bandwidth	6.4 eV	2.2 eV
Melting point	2730°C	1580°C
Microelectronics	HT-devices	Schottky diode
Optoelectronics	UV-diode	LED
Bearings etc.	Wear-resistance	Wear resistance

Fig. 1. Schematic representation of an IBAD-unit.

Ion bombardment is the key factor controlling film properties in the IBAD process. The ions impart substantial energy to the coating and coating/substrate interface, achieving the benefits of substrate heating (which generally provides a denser, more uniform film) without significantly heating the substrate material and degrading bulk properties. The ions also interact with coating atoms, driving them into the substrate and producing a graded material interface, which enhances adhesion. Due to these factors and compared to other synthesis processes of c-BN such as Chemical Vapor Deposition (CVD), IBAD features a higher adatom mobility, guarantees a better condensation of the layers, improves the layer-substrate adhesion, and facilitates chemical bonding.

The IBAD process is characterized by a layered deposition featuring specific crystallographic phases [1–3]. Typically, we have an initial amorphous phase of a thickness between 0.2 and 4 nm, then a layer of hexagonal boron nitride (h-BN) of a thickness between 2 and 7 nm, followed by a layer of c-BN whose thickness amounts to approximately 80% of the deposited film. The thickness of the different layers strongly depends on the ratio I/A of the arrival rates of the N- and B-atoms at the surface of the substrate.

As far as the co-deposition of fullerenes on silicon substrate is concerned, it has been shown [4,5] that thin SiC films, up to 1 μm thick, can be grown on (0 0 1) silicon substrates by C_{60} carbonization at rather low substrate temperatures around 800°C. The experimental equipment used for co-deposition of fullerenes is similar to the IBAD, except for the ion gun. Inside a typical vacuum chamber (10^{-9} mbar), the silicon wafer is mounted on a heater to keep the temperature of the sample constant. Fullerenes are produced in a BN crucible at the bottom of the chamber in the same manner as the boron atoms, controlling the deposition rate of fullerenes on the wafer by an appropriate sensor. Also, a graphite crucible for the evaporation of silicon is included to avoid the formation of holes under the SiC layer. With the inclusion of the new crucible, the SiC film is produced by the silicon atoms that reach the surface from the vapor and not from the substrate. The Si–C bond formation at rather low substrate temperatures can be explained by the condensation energy from the 60 carbon atoms forming the fullerene, which is released as the molecules hit the wafer surface and break apart.

The paper is organized as follows: In Section 2, we consider modeling and simulation of the production process described by molecular dynamics using Tersoff-type potentials whose parameters are determined by ab initio quantum mechanical calculations. Finally, in Section 3 we present visualizations of the numerical simulation results analyzing in detail the effect of different energies and rotational frequencies.

2. Modeling and simulation by molecular dynamics

Mathematical modeling of the processes described in the Introduction is performed by Molecular Dynamics (MD) simulations, a tool that can provide considerable physical insight into the origin of structural properties of materials. Its application to complex structures is limited by the associated computational requirements.

In molecular dynamics, the behavior of a system of N particles is modeled by Newton's equations of motion, describing the interatomic interaction with a proper empirical potential energy, $V(\mathbf{r}_1, \ldots, \mathbf{r}_N)$, as a function of the position vectors of all particles. By using suitable potentials with multibody functions, empirical MD simulation can considerably shorten the computation time while yielding physical properties with desirable accuracy.

For the present processes, suitable choices are Brenner- and Tersoff-type potentials (cf., e.g., [6–11]) which are of the form

$$V = \frac{1}{2} \sum_{i \neq j} V_{ij} = \frac{1}{2} \sum_{i \neq j} f_C(r_{ij})[f_R(r_{ij}) + b_{ij} f_A(r_{ij})]. \quad (2.1)$$

Here, $r_{ij} := |\mathbf{r}_i - \mathbf{r}_j|$, $1 \leqslant i \neq j \leqslant N$, and $f_C(r)$ is a cut-off function

$$f_C(r) := \begin{cases} 1, & r < R - D, \\ \frac{1}{2} - \frac{1}{2} \sin(\frac{\pi}{2} \frac{r-R}{D}), & R - D \leqslant r \leqslant R + D, \\ 0, & R + D < r, \end{cases} \quad (2.2)$$

whereas $f_A(r)$, $f_R(r)$ denote attractive and repulsive potentials, respectively, that decay exponentially with distance.

Moreover, the bond-order parameter b_{ij} is chosen as a monotonically decreasing function of the number of neighbors of the atoms i and j according to the bond-order-concept which states that the more neighbors an atom has, the weaker the bond to each neighbor:

$$b_{ij} := (1 + \beta^m \xi_{ij}^m)^{-1/2m}. \quad (2.3)$$

Here, ξ_{ij} is the effective coordination number given by

$$\xi_{ij} := \sum_{k \neq i,j} f_C(r_{ik}) g(\theta_{ijk}) \exp(\lambda_3^3 (r_{ij} - r_{ik})^3),$$

$$g(\theta) := 1 + \frac{c^2}{d^2} - \frac{c^2}{d^2 + (h - \cos\theta)^2}, \quad (2.4)$$

where θ_{ijk} represents the bond angle formed by the bond between atom i and atom j and the bond between atom j and atom k.

Parameters of the Tersoff potential are fitted both by using experimentally obtained data such as elasticity modules and lattice specific constants as well as with regard to structural energies (e.g., surface and defect energies) and interatomar forces computed by means of ab initio quantum mechanical calculations [10,11].

For the numerical integration we have used a standard symplectic integrator of order 2, commonly used in molecular dynamics, namely the Velocity Verlet algorithm (also known as Störmer–Verlet). This integrator was initially introduced to improve the numerical stability of the leap frog scheme, allowing an accurate and fast evaluation of the equation of motion. It has the form

$$\mathbf{r}_i(t + \Delta t) = \mathbf{r}_i(t) + \Delta t \, \mathbf{v}_i(t) + \frac{1}{2} \frac{(\Delta t)^2}{m_i} \mathbf{F}_i(t),$$

$$\mathbf{v}_i(t + \Delta t) = \mathbf{v}_i(t) + \frac{1}{2} \frac{\Delta t}{m_i}(\mathbf{F}_i(t) + \mathbf{F}_i(t + \Delta t)),$$

$$1 \leqslant i \leqslant N. \quad (2.5)$$

A specific experimental feature, which has to be considered in the simulation, is that during the deposition process the temperature of the substrate is kept constant. Indeed, the temperature is an essential process parameter that significantly influences the crystallographic structure. In the simulations, the interaction between the substrate, represented only by a small number of atoms, and ions with high energy would lead to an unrealistic heating of the substrate and a mechanism has to be included to represent the heat convection to the thermal bath.

The temperature T of a system of N particles, each particle having three degrees of freedom, is related to the kinetic energy E_k according to

$$E_k = \frac{3}{2} k_B N T, \quad (2.6)$$

where k_B is the Boltzmann constant. Therefore, the temperature stays constant if the same applies to the kinetic energy, which in terms of the velocities is given by

$$E_k = \frac{1}{2} \sum_{i=1}^{N} m_i \mathbf{v}_i^2. \quad (2.7)$$

Then, at each time step of the simulations the velocities $\mathbf{v}_i$ of the atoms located at the bottom layer, are rescaled by the factor

$$\alpha := \sqrt{\frac{E_k^*}{E_k}},$$

where E_k^* is given by (2.6) with the constant temperature T, and E_k is given by (2.7) with respect to the actually computed velocities $\mathbf{v}_i$ at that time level.

The rescaling is only performed for the velocities of the atoms in the lowest monolayer of the substrate, because it should not effect the interaction between the Si-atoms of the substrate and the impacted atoms. All Si-atoms above are only indirectly influenced by "thermal contact" with the bottom layer. This corresponds to a thermal coupling with an infinitely large heat bath.

To improve the computational time of the molecular dynamic simulation, we introduce the particle-in-cell method with the addition of a safety distance scheme [7]. In this way we restrict ourselves to the nearest neighbors concept in the sense that we neglect interatomic forces for distances $r_{ij} > r_C$, where r_C is some pre-specified cut-off radius.

3. Simulation results

The model validation and verification of the numerical results by comparison with available experimental data for the same experimental setup is an important issue in the molecular dynamics approach. Following the techniques outlined in Section 2, we have performed simulations for the c-BN synthesis and fullerene co-deposition. Specific interest has been devoted to the

question whether the simulation reveals the same structure of the layers and phase transitions, i.e., formation of hexagonal lattices and transition to cubic crystallographic structures [1–3], and the bursting of fullerene and redistribution of C-atoms in the SiC layer [4,5].

In c-BN synthesis, we fixed the substrate temperature at $600°$K, assuming a firing rate of 1000 fs for both B-atoms (0.1 eV) as well as N-ions (100 eV), and an arrival ratio I/A of 0.4 [14].

The crystallographic structure of h-BN is shown in Fig. 2. In the honeycomb-like layers B-atoms (big red) and N-atoms (small green) are connected with covalent bonds.

The hexagons of the different layers are ordered one upon another where below and above of each B-atom (resp. N-atom) there is an N-atom (resp. B-atom) of the neighboring layer. Within each layer, a B-atom is tied to three neighboring N-atoms by homeopolar bonds. Between the layers there only act weak van der Waals forces so that the layers can be easily split.

In the same figure, from left to right, we can see the transition from the hexagonal to the cubic phase at an initial and a more progressed stage. We clearly see that homeopolar bonds are formed between the B-atoms of a layer and the N-atoms of the two neighboring layers. Fig. 3 (right) shows the final cubic phase with a very dense packing of the layers where each B-atom (resp. N-atom) is connected to four N-atoms (resp. B-atoms) like the vertices of a tetrahedral grid.

As far as the fullerene co-deposition process is concerned, due to the small deposition rate ($0.1C_{60}/s$), in our simulation we have considered the arrival of only one fullerene molecule, analyzing the system for different translational (0.1–500 eV) and rotational (1–500 GHz) energies. The silicon wafer is modeled by an arrangement of $7 \times 7 \times 7$ Si atoms representing an area of 1.45×10^{-17} m^2. The fullerene initially is at a distance of 6.5 Si lattice constants above the surface with a certain velocity fixed to impact into the center of the Si wafer, forming an angle θ with it. As before, the atoms forming the bottom layer of the wafer are kept fixed and a thermal correction is performed. Otherwise, the initial speed of atoms is chosen at random, following Boltzmann distribution for an initial temperature of $1100°$K.

Fig. 3 shows the interaction between a fullerene molecule and the silicon crystal for different energy values. For low impact energies (<200 eV), the fullerene impinges on the surface with the C-atoms chemically bonded to it. In case of higher impact energies, the fullerene penetrates into the surface layer and bursts. In this case, atoms of the fullerene are completely embedded within the surface layer starting to mix with Si atoms. The size of the resulting crater depends on the impact energy, affecting only a few layers of the surface.

We also analyzed the effect of fullerene rotation during the interaction with the silicon surface. In a previous work, the rotational effect on the disintegration of an ideal fullerene (a symmetrical fullerene cluster) was studied [12]. It was found that the C_{60} molecule disintegrates when it is initially rotated with an angular velocity larger than ≈ 30 Thz. In our simulation this value was drastically reduced to about 800 GHz. We believe that this difference is due to the thermal effect introduced in our work through the initial random speed of carbon atoms given by Boltzmann probability distribution function.

How affect the molecular rotation the interaction between the C_{60} and the silicon surface? For low angular frequencies (<10 GHz) there are no apparent influence, no matter the value of the fullerene energy. The
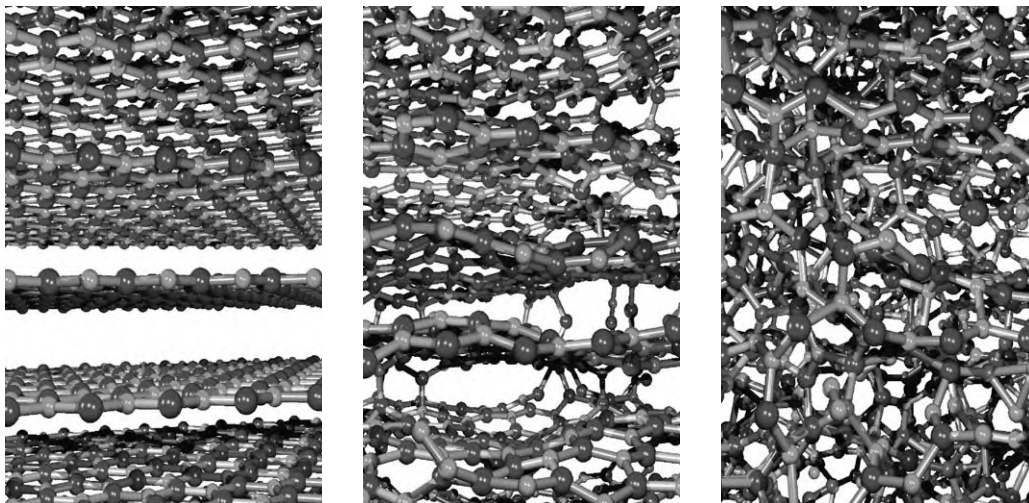

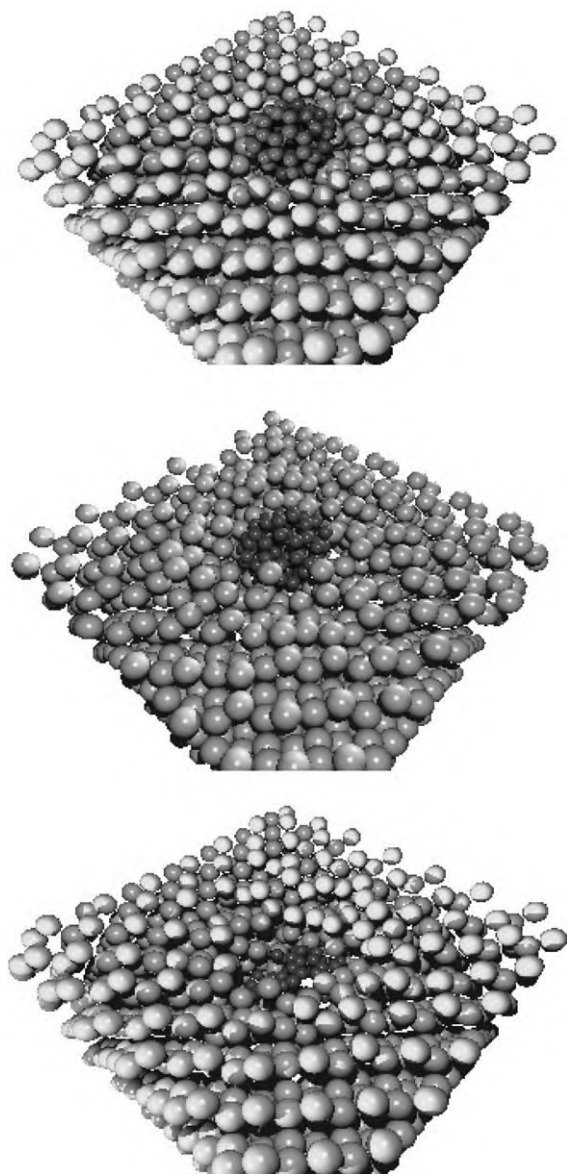Fig. 2. Formation of h-BN (left) and transition to c-BN (right).

Fig. 3. Impact of the fullerene molecule onto a silicon wafer for different energies (100 eV top, 250 eV center and 500 eV bottom).

Fig. 4. SiC crystallographic structure.

atoms before it stops. If the rotational frequency is high enough the fullerene bursts, spreading carbon atoms over the silicon surface in the direction of motion.

The fullerene velocity is perpendicular to the silicon surface in all the simulations described. If we decrease the impact angle the result is that expected: the fullerene tends to move over the surface in the same direction of the impact.

We finally studied the crystallographic structure of the SiC film produced by the bombarding the silicon wafer by carbon and silicon low energy atoms. We have performed simulations varying the fired rate between 600 and 3000 fs, and the impact energy between 0.1 and 0.5 eV for both atoms. In all the simulations the result is a disordered structure where the cubic bonds are clearly seen (Fig. 4).

Acknowledgements

consequence of higher frequencies in the fullerene impact depends on the arrival energy. For energies lower than 100 eV the fullerene start moving over the silicon surface. The range of the movement after the final stop depends on the initial frequency. For impact energies higher than 200 eV the are no changes in the final result. The hole produced in the silicon surface does not differ from the no-rotation case. An interesting situation occurs for intermediate impact energies. Because of the rotation, the fullerene molecule tends to move over the surface and can lose a couple of carbon

References

[1] Kester DJ, Ailey KS, Davis RF, More KL. Phase evolution in boron nitride thin films. J Mater Res 1993;8: 1213–6.

[2] Medlin DL, Friedmann TA, Mirkarimi PB, Rez P, Mills MJ, McCarty KF. Microstructure of cubic boron nitride thin films grown by ion-assisted pulsed laser deposition. J Appl Phys 1994;76:295–303.

[3] Yamashita H, Kuroda K, Saka H, Yamashita N, Watanabe T, Wada T. Cross-sectional transmission electron microscopy observations of c-BN films deposited on Si by ion-beam-assisted deposition. Thin Solid Films 1994;253:72–7.

[4] Volz K, Schreiber S, Zeitler M, Rauschenbach B, Stritzker B, Ensinger W. Structural investigations of silicon carbide films formed by fullerene carbonization of silicon. Surf Coat Technol 1999;122:101–7.

[5] Volz K, Schreiber S, Gerlach JW, Reiber W, Rauschenbach B, Stritzker B, Assmann W, Ensinger W. Heteroepitaxial growth of 3C-SiC on (1 0 0) silicon by C_{60} and Si molecular beam epitaxy. Mat Sci Eng A 2000;289: 255–64.

[6] Albe K. Computersimulation zu Struktur und Wachstum von Bornitrid. Doktorabeit: Forschungszentrum Rossendorf; 1998.

[7] Albe K, Möller W, Heinig K-H. Computer simulation and boron nitride. Radiat Eff Det Solids 1997;142:85.

[8] Brenner DW. Empirical potential for hydrocarbons for use in simulating the chemical vapor deposition of diamond films. Phys Rev B 1990;42:9458–71.

[9] Tersoff J. New empirical approach for the structure and energy of covalent systems. Phys Rev B 1988;37: 6991–7000.

[10] Tersoff J. Empirical interatomic potential for silicon with improved elastic constants. Phys Rev B 1989;38:9902–5.

[11] Tersoff J. Empirical interatomic potential for carbon with applications to amorphous carbon. Phys Rev Lett 1988;61:2879–82.

[12] Makino S, Oda T, Hiwatari Y. Classical molecular dynamics for the formation process of a fullerene molecule. J Phys Chem Solids 1997;58:1845–51.

[13] Bockstedte M, Kley A, Neugebauer J, Scheffler M. Density-functional theory calculations for polyatomic systems: electronic structure, static and elastic properties and ab initio molecular dynamics. Comput Phys Commun 1997;107:187.

[14] Hoppe RHW, Sibona G, Revnic A, Schweitzer D. Numerical simulation of ion beam assisted deposition of thin cubic boron nitride films. Comput Vis Sci, submitted.

[15] Zeuner M, Meichsner J, Neumann H, Scholze F, Bigl F. Design of ion energy distributions by a broad beam ion source. J Appl Phys 1996;80:611–22.